Density Functional Study on the C-H Bond Cleavage of Aldimine by a Rhodium(I) Catalyst

Kyunghwa Yoo, Chul-Ho Jun, Cheol Ho Choi,† and Eunji Sim*

Department of Chemistry and Institute for Nano-Bio Molecular Assemblies, Yonsei University, Seoul 120-749, Korea
**E-mail: esim@yonsei.ac.kr*
†*Department of Chemistry, Kyungpook National University, Daegu 702-701, Korea*
Received June 12, 2008

We investigated the C-H bond activation mechanism of aldimine by the [$RhCl(PPH_3)_3$] model catalyst using DFT B3LYP//SBKJC/6-31G*/6-31G on GAMESS. Due to their potential utility in organic synthesis, C-H bond activation is one of the most active research fields in organic and organometallic chemistry. C-H bond activation by a transition metal catalyst can be classified into two types of mechanisms: direct C-H bond cleavage by the metal catalyst or a multi-step mechanism via a tetrahedral transition state. There are three structural isomers of [$RhCl(PH_3)_2$] coordinated aldimine that differ in the position of chloride with respect to the molecular plane. By comparing activation energies of the overall reaction pathways that the three isomeric structures follow in each mechanism, we found that the C-H bond activation of aldimine by the [$RhCl(PH_3)_3$] catalyst occurs through the tetrahedral intermediate.

Key Words : Density functional theory, C-H cleavage, Catalytic reaction, Reaction mechanism, GAMESS

Introduction

C-H bond activation is one of current interest in organometallic chemistry.[1] In particular, hydroacylation, the catalytic transformation of an aldehyde or a 1-alkene to the corresponding ketone, has been a focus in synthetic organic chemistry due to its atom economical efficiency.[2] Chelation-assisted hydroacylation using 2-amino-3-picoline is one of the preferred hydroacylation methods because it allows suppression of side reactions such as decarbonylation,[3] due to the involvement of an aldimine intermediate *in-situ* generated from aldehyde and 2-amino-3-picoline. The chelation-assisted C-H bond cleavage of aldimine by a transition metal is considered an important step in this catalytic reaction. Previously, Suggs developed and showed the stoichiometric and catalytic cleavage of the C-H bond in this aldimine intermediate which was prepared by condensation of benzaldehyde and 2-amino-3-picoline.[4] Nevertheless, a plausible mechanism of the C-H bond cleavage of aldimine by Rh(I) complexes has not yet been determined, though many theoretical studies on the C-H bond cleavage by transition metal complexes have been reported.[5] Therefore, in this paper we focus on the mechanism of C-H bond cleavage in aldimine by a rhodium(I) complex.

Two possible mechanisms for chelation-assisted C-H bond cleavage by transition metal complexes have been proposed

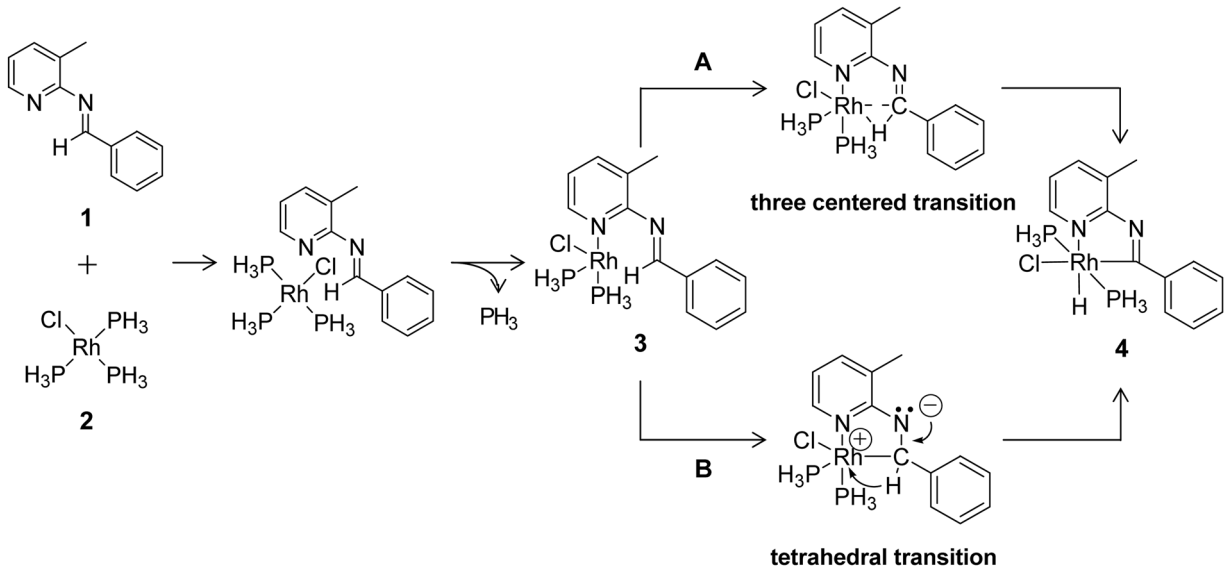

Scheme 1. C-H bond activation mechanism of aldimine by Rh catalyst (A: direct C-H bond cleavage by insertion of the catalyst, B: tetrahedral transition state by breaking C=N double bond within imine).

as shown in Scheme 1: (A) direct C-H bond cleavage by the transition metal catalyst[6] or (B) a multi-step mechanism via a tetrahedral transition state,[7] *i.e.*, initial electron transfer from the metal catalyst to the C=N double bond of aldimine and subsequent hydrogen migration from the C-H bond of the resulting tetrahedral transition state to the metal catalyst. A carbon atom in the transition state in mechanism A has a three-centered structure, while in mechanism B it has a tetrahedral structure. In the present study, we aim to demonstrate the reaction mechanism from complex **3** to complex **4** in Scheme 1 by means of density functional theory (DFT) calculation, in order to elucidate the C-H bond cleavage of aldimine **1** by rhodium(I) complex **2**.

Following a brief explanation of calculation procedures in Section 2, we will discuss both the mechanism for direct Rh(I)-insertion into the C-H bond and the multi-step mechanism in Section 3. Results are discussed with reference to potential energy determination, and the lowest overall activation reaction pathway is determined. Finally, concluding remarks are provided in Section 4.

Calculation Procedure

Geometries of the reactants, intermediates, transition states and products of Scheme 1 were optimized using the DFT with the B3LYP exchange-correlation functional and hybrid basis sets. The SBKJC effective core potential basis set that avoids redundant evaluation of core electrons in every iteration step was adopted for the transition metal Rh.[8] The 6-31G basis set was applied to H, while the 6-31G* basis set was used for the remaining atoms. Normal coordinate analysis has been performed for all stationary points to characterize transition states (one imaginary frequency) and equilibrium structures (no imaginary frequencies). Intrinsic reaction coordinate calculations, starting at transition structures, were performed to determine pathways between reactants and products as well as corresponding transition states. All calculations and structural analyses were performed using the GAMESS (General atomic and molecular electronic structure system) program.[9] All the energies presented in this study include zero-point energies. All calculations were performed in gas phase. Solvent effect was assumed to be negligible, since experiments were conducted in solution using a nonpolar solvent, toluene.

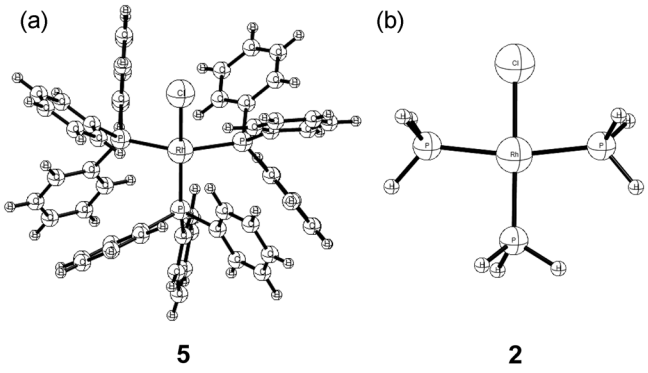

Figure 1. (a) Experimentally determined $[Rh(PPh_3)_3Cl]$ complex structure[13] and (b) optimized $[Rh(PH_3)_3Cl]$ complex structure.

The Wilkinson catalyst, **5**, was modeled as $[Rh(PH_3)_3Cl]$, **2**, by substituting hydrogen atoms for bulky phenyl groups. This model has been widely used in theoretical studies and has been shown to provide reliable conclusions and scientific insights.[10-12] Since the x-ray structure of $[Rh(PPh_3)_3Cl]$ has been established by Bennett and Donaldson[13] (as shown in Fig. 1), we constructed an initial structure of $[Rh(PH_3)_3Cl]$ based on x-ray parameters of $[Rh(PPh_3)_3Cl]$ and computed an optimized structure using DFT B3LYP//SBKJC/6-31G*/6-31G with GAMESS. $[Rh(PPh_3)_3Cl]$ crystallizes into red and orange allotropic forms, differing in the relative positions of the phenyl groups. For this study, parameters of the red form used in heat conduction experiments were selected.[3] Figure 1 shows the structures of $[Rh(PH_3)_3Cl]$ and $[Rh(PPh_3)_3Cl]$. Geometric parameters of theoretical $[Rh(PH_3)_3Cl]$ and experimental(x-ray) $[Rh(PPh_3)_3Cl]$ are listed in Table 1. Note that the bond lengths in **2** and **5** are very similar except for a slight discrepancy in Cl-Rh-P and P-Rh-P angles. The discrepancy is likely to be associated with the R group present in PR_3 phosphines. These results indicate that the $Rh(PH_3)_3Cl$ model and computational method provide a reasonable assessment of geometry.

In the reaction of aldimine **1** with the catalyst complex **2**, one of the phosphine ligands in **2** is initially dissociated, and then the nitrogen in pyridine of **1** is coordinated to the vacant site of the catalyst. Depending on the position of the dissociated phosphine ligand, there exist three structural

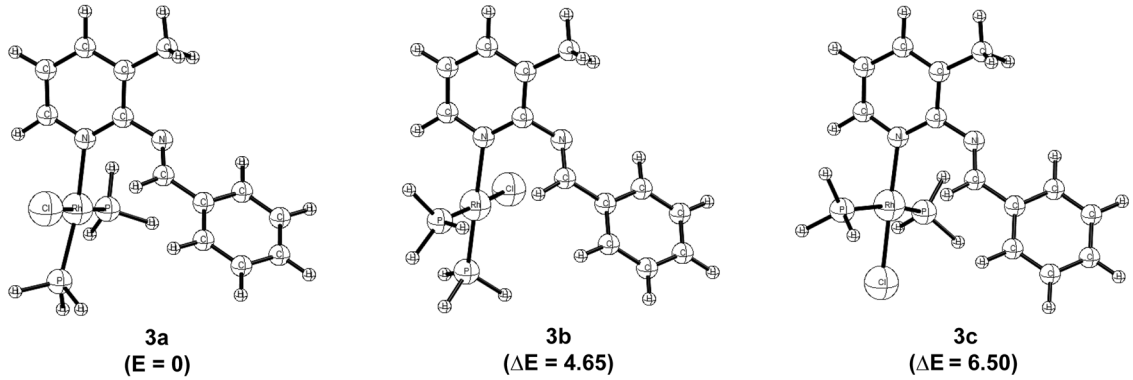

Figure 2. Structures and relative energies of **3a**, **3b** and **3c**.

Table 1. Geometry parameters of calculated [$Rh(PH_3)_3Cl$] and experimental (x-ray) parameters of [$Rh(PPh_3)_3Cl$][13]

Parameter, Å or deg	$Rh(PPh_3)_3Cl$ (x-ray)	$RhCl(PH_3)_3$ (calculation)
Rh-Cl	2.376	2.412
Rh-P	2.214	2.242
Rh-P	2.322	2.306
Rh-P	2.334	2.314
Cl-Rh-P	156.2	179.4
P-Rh-P	152.8	168.3

isomers of **3** as shown in Figure 2. Herein, **3a** and **3b** bear a strong resemblance in their structure while that of **3c** is completely different. Nevertheless, **3a** and **3b** can not be obtained through conformational isomerization since the phenyl group hinders the rotation of C-Rh bond. Therefore we consider the three structures of the compound **3** independently as the reactant. We examined the relative stability of the three isomers, **3a**, **3b** and **3c**, and found that

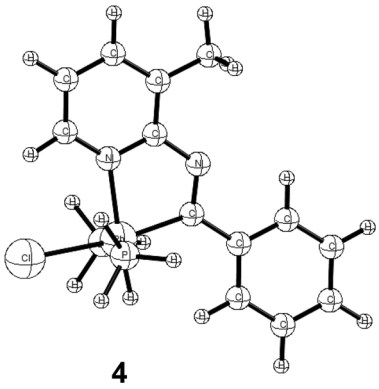

Figure 3. Optimized structure of iminoacylrhodium(III) hydrid which is based on the structure established by ^{1}H NMR analysis[4].

the energy of **3a** is lower than those of **3b** and **3c** by 4.6 and 6.5 kcal/mol, respectively. Since **3a**, **3b** and **3c** are potential intermediates in this reaction, there are several possible pathways for C-H bond cleavage. Thus, we investigated all

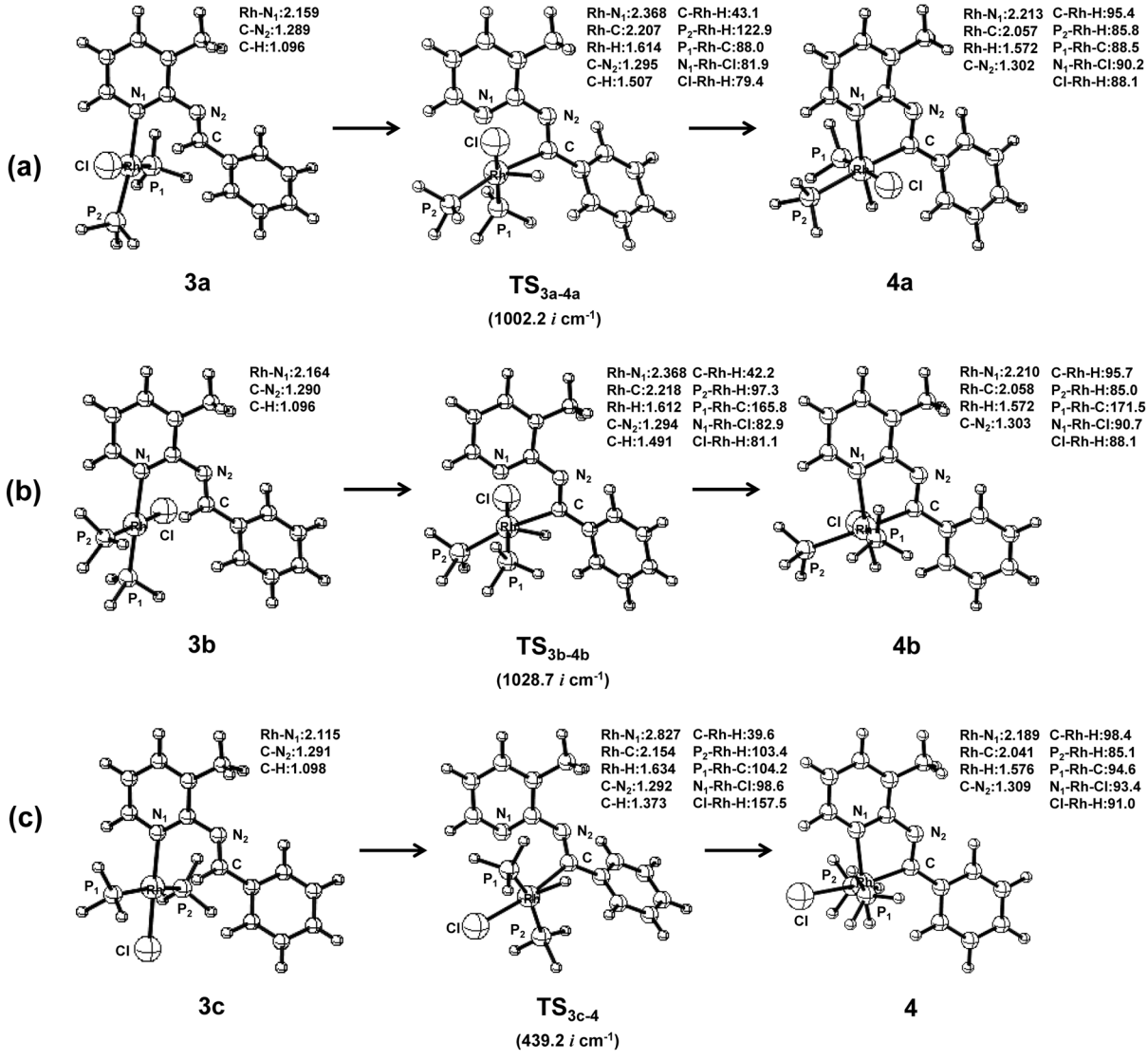

Figure 4. Reaction pathways of (a) **3a**, (b) **3b** and (c) **3c** following the Rh insertion mechanism.

possible reaction pathways starting from these three structural isomers despite the fact that **3a** is the most stable intermediate.

By cleaving a C-H bond of **3** through either of the two mechanisms, A or B in Scheme 1, a hydrogen atom in **3** migrates to Rh, forming a iminoacylrhodium(III) hydrid **4**. Complex **4** is a highly stable intermediate in the chelation-assisted hydroacylation reaction, which can be isolated and examined by ^{1}H NMR analysis. According to the ^{1}H NMR study, the hydrogen atom attached to the rhodium metal is located in the same plane as aldimine, which is on the opposite side of the nitrogen in pyridine as shown in Figure 3.[4]

Results and Discussion

A. Mechanism of direct Rh-insertion into the C-H bond through a three-centered transition state. To identify direct C-H bond cleavage of aldimine by the rhodium(I) metal center, structural changes and energies were tracked as C=N bond distance was increased while decreasing Rh-C and Rh-H distances which mimics the natural process. Normal coordinate analyses starting from all three isomers were also performed.

In Figure 4(a), starting from **3a**, $\mathbf{TS_{3a\text{-}4a}}$ is formed through three-centered Rh-H-C with a large activation energy of 41.88 kcal/mol. When the Rh metal is inserted into the C-H bond of aldimine as in $\mathbf{TS_{3a\text{-}4a}}$, an Rh-N bond in which the N atom is in pyridine moiety, is stretched out from 2.16 Å to 2.37 Å and Rh-H and Rh-C bonds are formed with lengths of 1.61 Å and 2.21 Å, respectively. As Rh-H bond lengths were further decreased as in **4a**, the Rh-N coordination bond was separated by 2.21 Å. The reaction pathway from an unstable intermediate **4a** to stable **4** was also examined. However, our calculations showed that the transition from **4a** to **4** is possible only with the breakage of bonds such as Rh-PH_3, Ph-Cl and others. Since bond breaking requires much more energy than the rearrangement of atoms via rotation, we did not pursue the rest of this reaction pathway.

Starting from the **3b** structure, an intermediate **4b** is formed through a transition state $\mathbf{TS_{3b\text{-}4b}}$ with an activation energy of 42.53 kcal/mol as shown in Figure 4(b). Following the pathway, Rh-H-C forms a triangular structure as the Rh-N bond is stretched. In $\mathbf{TS_{3b\text{-}4b}}$, Rh-C, Rh-H and Rh-N bond lengths are 2.22 Å, 1.61 Å and 2.37 Å, respectively. Intermediate **4b** is less stable than **3b** by 7.30 kcal/mol. Bond breaking is also necessary to transform **4b** to **4**. Therefore, the rest of the pathway was not explored.

Unlike **3a** and **3b**, the reaction from **3c** to **4** proceeds through a single transition state, $\mathbf{TS_{3c\text{-}4}}$, with an energy barrier of 31.16 kcal/mol, is shown in Figure 4(c). At $\mathbf{TS_{3c\text{-}4}}$, the Rh metal inserts into the C-H bond with a triangular structure in which Rh-H distance decreases to 1.63 Å and a Rh-C bond is formed at a distance of 2.15 Å. On the other hand, the Rh-N length is increased to 2.83 Å and the C-H bond is essentially broken at 1.37 Å in length. The iminoacylrhodium(III) hydrid **4** is 7.83 kcal/mol more stable than **3c**.

Owing to direct C-H bond cleavage by the catalyst, all isomer structures of **3** have an Rh-H-C three-centered transition state which results from the insertion of the Rh metal center into the C-H bond. While **3c** is able to form the stable iminoacylrhodium(I) hydride intermediate **4** through a single transition state $\mathbf{TS_{3c\text{-}4}}$, isomers **3a** and **3b** cannot form a stable intermediate **4** without bond breaking and reforming of Cl, two-PH_3, or H groups. Following mechanism of direct Rh-insertion into the C-H bond through a three-centered transition state, energy changes of **3a**, **3b** and **3c** are summarized in Table 2, respectively.

Table 2. Energy changes of **3a**, **3b** and **3c** following mechanism of direct Rh-insertion into the C-H bond through a three-centered transition state

Initial Structure	$\Delta E^{\dagger}$	ΔE
3a	41.88	6.68
3b	42.53	7.30
3c	31.16	7.83

$\Delta E^{\dagger} = E_{TS} - E_i$, $\Delta E = E_f - E_i$. E_{TS}: energy of the transition state. E_i: energy of the initial structure. E_f: energy of the final structure

B. Multi-step mechanism through a tetrahedral transition state. As illustrated in Scheme 1, when electrons of the rhodium(I) metal center are donated to the carbon of imine in **3**, the double bond between carbon and nitrogen is converted into a partial single bond while a new Rh-C bond is formed. We performed normal coordinate analysis using the GAMESS code, starting from the three isomers **3a**, **3b**, and **3c**.

Figure 5(a) presents the overall reaction pathway from **3a**. The intermediate **4a'** is formed from **3a** through the transition state $\mathbf{TS_{3a\text{-}4a'}}$ where the Rh-H bond formation and C-H bond breaking are synchronously in progress. In $\mathbf{TS_{3a\text{-}4a'}}$, the Rh-C distance is as short as Rh-C bond length, *i.e.*, a new Rh-C bond is nearly formed. In the course of the transformation from **3a** to $\mathbf{TS_{3a\text{-}4a'}}$, the sp^2 carbon of imine is transformed into a sp^3 carbon with a tetrahedral structure having Rh, N, a phenyl group, and an H atom at the vertices. Then, as the Rh-H bond length is decreased with increasing C-H bond length, Rh-H-C forms a triangular structure. The activation energy for this pathway is 17.71 kcal/mol and the energy of **4a'** is higher than that of **3a** by 3.53 kcal/mol. Note that **4a'** does not adopt the structure of the stable iminoacylrhodium(III) hydrid **4** established by ^{1}H NMR analysis. For the conformation of the stable structure (**4**), **4a'** undergoes rearrangements through two more transition states, $\mathbf{TS_{4a'\text{-}4a''}}$ and $\mathbf{TS_{4a''\text{-}4}}$. In this second reaction step, **4a''** is formed by changing the positions of Cl and two-PH_3 at **4a'** through $\mathbf{TS_{4a'\text{-}4a''}}$. The position of H does not change at this stage; however, PH_3 migrates easily by decreasing the C-Rh-H angle from 87.1° to 68°. The activation barrier is calculated to be 29.04 kcal/mol and **4a''** is 2.69 kcal/mol less stable than **4a'**. The third step begins from **4a''** to get to **4** through $\mathbf{TS_{4a''\text{-}4}}$ with an energy barrier of 19.49 kcal/mol. The energy of **4,** a stable iminoacylrhodium(III) hydrid, is 7.69 and 1.47 kcal/mol lower than those of **4a''** and **3a**, respectively.

When starting from **3b**, the intermediate **4b'** is formed

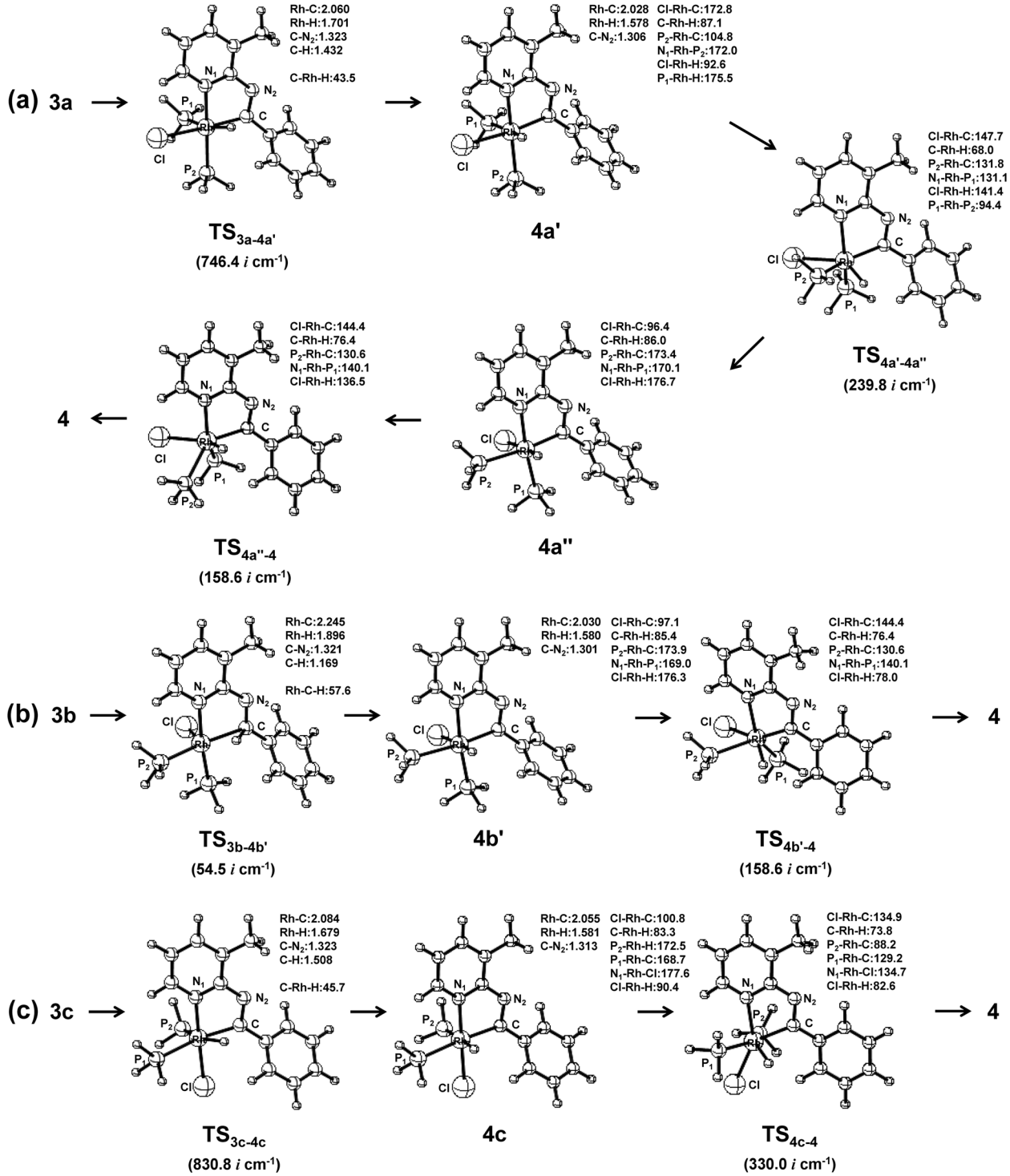

Figure 5. Reaction pathways of (a) **3a**, (b) **3b** and (c) **3c** following the multi-step mechanism.

through a transition state $\mathbf{TS_{3b\text{-}4b'}}$ with an activation energy of 17.36 kcal/mol (Fig. 5(b)). As the Rh atom approaches the carbon atom in the imine group of **3b**, a Rh-C bond is formed at $\mathbf{TS_{3b\text{-}4b'}}$ bearing a tetrahedral carbon with Rh, N, H and the phenyl group at vertices. The Rh-H-C then forms a triangular structure by shortening the Rh-H distance while lengthening the C-H bond. Finally, the H atom migrates from the carbon of imine to the Rh metal center. The energy of **4b'** is higher than that of **3b** by 1.98 kcal/mol. The stable hydride complex **4** is formed by rotations of Cl, H and two-PH_3 in **4b'**. The energy barrier for $\mathbf{TS_{4b'\text{-}4}}$ from **4b'** is 19.08 kcal/mol while **4** is more stable than **4b'** by 8.10 kcal/mol.

Finally, in the case of the **3c** isomer, **3c** is converted to the intermediate **4c** through the transition state $\mathbf{TS_{3c\text{-}4c}}$. During the transformation from **3c** to **4c**, a tetrahedral transition state is generated at the carbon of imine. Then, the Rh-H-C

Table 3. Energy changes of **3a**, **3b** and **3c** following multi-step mechanism through a tetrahedral transition state

Initial Structure	$\Delta E_1^{\dagger}$	ΔE_1	$\Delta E_2^{\dagger}$	ΔE_2	$\Delta E_3^{\dagger}$	ΔE
3a	17.71	3.53	32.57	6.22	25.71	−1.47
3b	17.36	1.98	21.07	–	–	−6.11
3c	13.57	3.54	42.00	–	–	−7.95

$\Delta E_n^{\dagger} = E_{n\text{-}TS} - E_i$, $E_n = E_{n\text{-}int.} - E_i$, $\Delta E = E_f - E_i$. $E_{n\text{-}TS}$: energy of the n^{th} transition state. E_i: energy of the initial structure. $E_{n\text{-}int.}$: energy of the n^{th} intermediate structure. E_f: energy of the final structure

forms a triangular structure by shortening the Rh-H distance while lengthening the C-H bond. The activation energy of $\mathbf{TS_{3c\text{-}4c}}$ is 13.57 kcal/mol. The energy of **4c** is higher than that of **3c** by 3.54 kcal/mol. As shown in Figure 5(c), **4** is formed from the migration of Cl, H and two-PH_3 in **4c**. The energy of **4**, which is formed through $\mathbf{TS_{4c\text{-}4}}$ with an activation energy of 38.46 kcal/mol, is lower than that of **4c** by 11.49 kcal/mol.

Throughout the multi-step C-H bond cleavage mechanism which involves electron-donation of the electron-rich rhodium(I) metal center to the carbon atom of imine, we observed that the carbon atom of imine commonly forms a tetrahedral structure with Rh, N, H, and the phenyl group at vertices, regardless of the starting isomeric structure of **3**. From the tetrahedral transition structure, then, Rh-H-C forms a triangular structure as Rh-H distance is further decreased and C-H distance increased. Following multi-step mechanism through a tetrahedral transition state, energy changes of **3a**, **3b** and **3c** are summarized in Table 3, respectively.

C. Overall C-H bond activation pathway. By comparing the two reaction pathways (A and B) for all three geometrical isomers, we identified a single transition state $\mathbf{TS_{3c\text{-}4}}$ (activation energy of 31.16 kcal/mol) from **3c** to **4** that acts through a direct C-H bond cleavage mechanism (Fig. 6). The reaction pathways from **3a** and **3b** cannot form a stable iminoacylrhodium(III) hydrid structure. Furthermore, the energy barriers considered stability of reactants for $\mathbf{TS_{3a\text{-}4a}}$ and $\mathbf{TS_{3b\text{-}4b}}$ are almost 5 kcal/mol higher than that of $\mathbf{TS_{3c\text{-}4}}$. However, we also found that stable iminoacylrhodium(III) hydrid **4** can be formed from **3a**, **3b** and **3c** through multi-

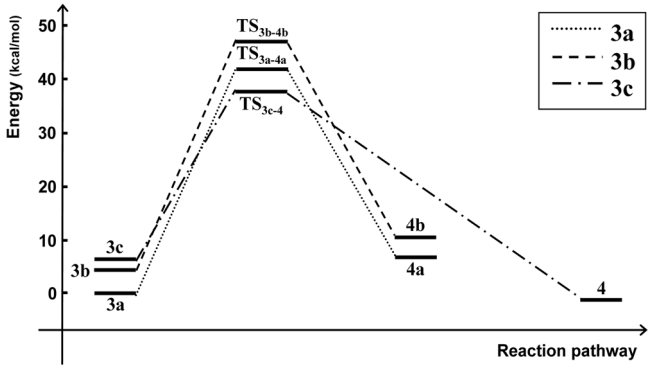

Figure 6. Potential energy profiles of reaction pathways following the Rh insertion mechanism.

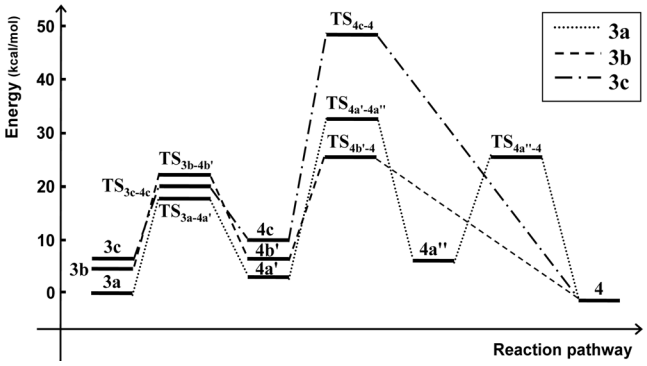

Figure 7. Potential energy profiles of reaction pathways following the multi-step mechanism.

step transition states involving tetrahedral intermediates by electron transfer and subsequent positional rearrangements of hydride, Cl, and PH_3 (Fig. 7). The energy of the iminoacylrhodium(III) hydrid **4** is 1.47, 6.11 and 7.95 kcal/mol lower than those of **3a**, **3b** and **3c**, respectively. Through the multi-step mechanism, the highest activation energy for **3a** is 32.57 kcal/mol for $\mathbf{TS_{4a'\text{-}4a''}}$ while that for **3b** corresponds to $\mathbf{TS_{4b'\text{-}4}}$ (21.07 kcal/mol) and for **3c** to $\mathbf{TS_{4c\text{-}4}}$ (42.00 kcal/mol).

Based on the above results, we conclude that the overall reaction mechanism for the stable iminoacylrhodium(III) hydrid reveals that the C-H bond activation of aldimine by a Rh catalyst takes place through the tetrahedral intermediate by the multi-step pathway of **3b**.

Concluding Remarks

This article presents a theoretical investigation of two C-H bond cleavage mechanisms of aldimine by a Rh catalyst: (1) direct C-H bond cleavage by the metal catalyst or (2) multi-step electron transfer C-H bond cleavage through a tetrahedral transition state. We found that there are three structural isomers of $[Rh(PH_3)_2Cl]$ coordinated aldimine owing to the position of Cl with respect to the molecular plane. Therefore, we performed simulations of overall reaction for all three isomers with each of the two mechanisms. The C-H bond activation pathways in which electron transfer occurred resulted in tetrahedral carbon structures with Rh, N, H, and the phenyl group. In contrast, direct C-H bond cleavage pathways resulted in a three-centered carbon structure with Rh and H. The most probable reaction pathway, which has the lowest activation energy in overall reaction, is the electron transfer pathway of **3b**. Thus, C-H bond activation of aldimine by a Rh catalyst occurs through a multi-step electron transfer mechanism with a tetrahedral transition state.

Acknowledgments. This work was supported by the Korea Science and Engineering Foundation (R01-2007-000-11831-0, ES). YK thanks the fellowship of the BK21 program from the Ministry of Education and Human Resources Development.

References

1. (a) Arndtsen, B. A.; Bergman, R. G.; Mobley, T. A.; Peterson, T. H. *Acc. Chem. Res.* **1995**, *28*, 154. (b) Niu, S.; Hall, M. B. *Chem. Rev.* **2000**, *100*, 353. (c) Shilov, A. E.; Shul'pin, G. B. *Chem. Rev.* **1997**, *97*, 2879. (d) Dyker, G. *Angew. Chem. Int. Ed.* **1999**, *38,* 1698. (e) Kakiuchi, F.; Murai, S. *Acc. Chem. Res.* **2002**, *35*, 826. (f) Kakiuchi, F.; Chatani, N. *Adv. Synth. Catal.* **2003**, *345*, 1077.
2. (a) Kondo, T.; Akazome, M.; Tsuji, Y.; Watanabe, Y. *J. Org. Chem.* **1990**, *55*, 1286. (b) Lenges, C. P.; White, P. S.; Brookhart, M. *J. Am. Chem. Soc.* **1998**, *120*, 6965. (c) Kondo, T.; Hiraishi, N.; Morisaki, Y.; Wada, K.; Watanabe, Y.; Mitsudo, T. *Organometallics* **1998**, *17*, 2131. (d) Tanaka, M.; Imai, M.; Yamamoto, Y.; Tanaka, K.; Shimowatari, M.; Nagumo, S.; Kawahara, N.; Suemune, H. *Org. Lett*. **2003**, *5*, 1365. (e) Kokubo, K.; Matsumasa, K.; Miura, M.; Nomura, M. *J. Org. Chem*. **1997**, *62*, 4564.
3. (a) Jun, C.-H.; Lee, H.; Hong, J.-B. *J. Org. Chem.* **1997**, *62*, 1200. (b) Jun, C.-H.; Huh, C.-W.; Na, S.-J. *Angew. Chem. Int. Ed.* **1998**, *37*, 145. (c) Jun, C.-H.; Hong, J.-B. *Org. Lett*. **1999**, *1*, 887. (d) Jun, C.-H.; Lee, H.; Hong, J.-B.; Kwon, B.-I. *Angew. Chem. Int. Ed*. **2002**, *41*, 2146. (e) Jun, C.-H.; Lee, H.; Hong, J.-B. *Angew. Chem. Int. Ed.* **2000**, *39*, 3070. (f) Jun, C.-H.; Moon, C. W.; Lee, D.-Y. *Chem. Eur. J.* **2002**, *8*, 2422. (g) Jun, C.-H. Lee, H.; Hong, J.-B.; Kwon, B.-I. *Angew. Chem. Int. Ed.* **2002**, *41*, 2146-2147. (h) Park, Y. J.; Kwon, B.-I.; Ahn, J.-A.; Lee, H.; Jun, C.-H. *J. Am. Chem. Soc.* **2004**, *126*, 13892-13893. (i) Jo, E.-A.; Jun, C.-H. *Eur. J. Org. Chem.* **2006**, 2504-2507.
4. Suggs, J. W. *J. Am. Chem. Soc.* **1979**, *101*, 489.
5. (a) Heiberg, H.; Gropen, O.; Swang, O. *Int. J. Quantum Chem.* **2003**, *92*, 391. (b) Broclawik, E.; Haber, J.; Piskorz, W. *Chem. Phys. Lett.* **2001**, *333*, 332. (c) Wiedemann, S. H.; Lewis, J. C.; Ellman, J. A.; Bergman, R. G. *J. Am. Chem. Soc.* **2006***, 128*, 2452. (d) Yoshizawa, K.; Shiota, Y.; Yamabe, T. *Organometallics* **1998**, *17*, 2825. (e) Jazzar, R. F. R.; Varrone, M.; Burrows, A. D.; Macgregor, S. A.; Mahon, M. F.; Whittlesey, M. K. *Inorg. Chim. Acta* **2006**, *359*, 815.
6. Crabtree, R. H. *Chem. Rev.* **1985**, *85*, 245.
7. (a) Markies, B. A.; Wijkens, P.; Kooijman, H.; Spek, A. L.; Boersma, J.; van Koten, G. *J. Chem. Soc., Chem. Commun.* **1992**, 1420. (b) Gozin, M.; Weisman, A.; Ben-David, Y.; Milstein, D. *Nature* **1993**, *364*, 600. (c) van der Boom, M. E.; Minstein, D. *Chem. Rev.* **2003**, *103*, 1759. (d) Vigalok, A.; Milstein, D. *Acc. Chem. Res.* **2001**, *34*, 798.
8. Use Stevens, Basch, Krauss, Jasien, Cundari potentials for all heavy atoms (Li-Rn are available). (a) Stevens, W. J.; Basch, H.; Krauss, M. *J. Chem. Phys.* **1984**, *81*, 6026. (b) Stevens, W. J.; Krauss, M.; Basch, H.; Jasien, P. G. *Can. J. Chem.* **1992**, *70*, 612. (c) Cundari, T. R.; Stevens, W. J. *J. Chem. Phys.* **1993**, *98*, 5555.
9. Schmidt, M. W.; Baldridge, K. K.; Boatz, J. A.; Elbert, S. T.; Gordon, M. S.; Jensen, J. H.; Koseki, S.; Matsunaga, N.; Nguyen, K. A.; Su, S. J.; Windus, T. L.; Dupuis, M.; Montgomery, J. A. J. *Comput. Chem.* **1993**, *14*, 1347.
10. (a) Musaev, D. G.; Mebel, A. M.; Morokuma, K. *J. Am. Chem. Soc.* **1994**, *116*, 10693. (b) Dorigo, A. E.; von Rague-Schleyer, P. *Angew. Chem., Int. Ed. Engl.* **1995**, *34*, 115. (c) Widauer, C.; Grützmacher, H.; Ziegler, T. *Organometallics* **2000**, *19*, 2097. (d) Liu, D.; Lin, Z. *Organometallics* **2002**, *21*, 4750.
11. (a) Cui, Q.; Musaev, D. G.; Morokuma, K. *Organometallics* **1997**, *16*, 1355. (b) Cui, Q.; Musaev, D. G.; Morokuma, K. *Organometallics* **1998**, *17*, 742. (c) Matsubara, T.; Maseras, F.; Koga, N.; Morokuma, K. *J. Phys. Chem.* **1996**, *100*, 2573.
12. (a) Sumimoto, M.; Iwane, N.; Takahama, T.; Sakaki, S. *J. Am.Chem. Soc.* **2004**, *126*, 10457. (b) Lam, W. H.; Lam, K. C.; Lin, Z.; Shimada, S.; Perutz, R. N.; Marder, T. B. *Dalton Trans*. **2004**, 1556. (c) Tamura, H.; Yamazaki, H.; Sato, H.; Sakaki, S. *J. Am. Chem. Soc.* **2003**, *125*, 16114.
13. Bennet, M. J.; Donaldson, P. *Inorg. Chem.* **1977**, *16*, 655.